International Journal of Refrigeration 131 (2021) 119–128

Contents lists available at ScienceDirect

International Journal of Refrigeration

journal homepage: www.elsevier.com/locate/ijrefrig

Refrigerant maldistribution in brazed plate heat exchanger evaporators. Part A: Testing campaign and experimental results

Emilio Navarro-Peris[a,*], Lucas Alvarez-Piñeiro[a], Paloma Albaladejo[a], Lena Schnabel[b], Jose M Corberan[a]

[a] Energy Engineering Institute, Universitat Politecnica de Valencia, Valencia, Spain
[b] Fraunhofer Institute for Solar Energy Systems, Freiburg, Germany

ARTICLE INFO

Article history:
Received 18 August 2020
Revised 3 April 2021
Accepted 6 April 2021
Available online 14 July 2021

Keywords:
Brazed plate heat exchanger
Evaporator
Refrigerant maldistribution
Efficiency

ABSTRACT

The refrigerant distribution in a brazed plate heat exchanger evaporator with distributor has been studied with a thermographic camera working under different conditions of inlet vapor quality, superheat, and water temperature drop. The thermographies have shown a clear uneven thermal distribution except when superheat is null. In most of the cases, they show that a great part of the liquid accumulates at the end channels of the evaporator. The degradation of the evaporator performance is higher when the water temperature drop has a similar or higher value than the superheat. On the other hand, when the superheat is significantly higher than the water temperature drop, the evaporator performance is very similar to situations in which there is an even distribution of the refrigerant. The registered evaporation temperatures are much lower for the case of 13 K of water temperature drop, highlighting the importance of the influence of this parameter on the evaporator performance. This research is described in two parts, Part A (present paper) including the description of the experimental campaign, the obtained experimental results and the results discussion and Part B including an analysis of the degradation of the evaporation temperature due to the refrigerant maldistribution as well as a deeper analysis of the registered temperatures and of the causes for the great degradation observed when the water temperature drop is increased.

Mauvaise distribution du frigorigène dans les évaporateurs d'échangeurs de chaleur à plaques

Mots-clés: Échangeur à plaques brasées; Évaporateur; Mauvaise distribution du frigorigène; Rendement

1. Introduction

Refrigerant maldistribution in evaporators is a well-known problem that could reduce significantly the performance of this component affecting negatively the global system efficiency, therefore it has been studied in the Literature for different heat exchangers typologies.

Some research has been dedicated to the characterization of the two-phase flow distribution when the flow is divided is several parts. For instance, (Vist and Pettersen, 2004) investigated the vapor quality distribution in heat exchanger manifolds, concluding that thermal performance can be significantly degraded due to liquid/vapor maldistribution. From their observations, vapor is taken out in the first channels when the inlet quality was low ($x = 0.11$) but distributes evenly in the first channels when quality is increased. However, no mention about the superheat in the evaporator during the measurements was made.

The refrigerant maldistribution can be very different depending on the flow pattern developed at the distributor. Flow visual-

* Corresponding author.
E-mail address: emilio.navarro@iie.upv.es (E. Navarro-Peris).

https://doi.org/10.1016/j.ijrefrig.2021.04.002

Nomenclature

BPHE	Brazed Plate Heat Exchanger
dTw	Water temperature drop across the evaporator (K)
$\dot{m}$	Mass flowrate (kg s^{-1})
PHE	Plate Heat Exchanger
SH	Superheat (K)
T	Temperature (°C)
T_{evap}	Evaporation temperature (°C)
T_{cond}	Condensation temperature (°C)
x	Vapor quality (-)

Subscripts

in	inlet
w	water
ref	refrigerant

ization in microchannels before entering the evaporator channels recognized two patterns: churn and separated flow. As it is commented in (Zou and Hrnjak, 2013) churn flow occurs when liquid and vapor phase are homogeneously mixed, whereas in separated flow, the different layers of vapor and liquid are perfectly separated. (Madanan et al., 2018) investigated the two-phase flow distribution of an air/water mixture from a U-type manifold into six and eight parallel horizontal mini-channels. The vapor phase distribution resulted to be dependent on the flow regime. A monotonic decrease was observed in case of slug flow and six channels, while oscillations occurred for the experiments with eight channels and plug flow.

In order to reduce the penalty of this problem in fin and tube evaporators some strategies have been employed following one of these two approaches:

1 Separating liquid and vapor and then distributing each one separately.
2 Generating a churn flow with a very good mixing of both phases and then introducing a distributor with a high pressure drop, avoiding in that way that the distribution could be altered by the different pressure drop generated along the different evaporator channels/circuits, due to differences in the inlet vapor quality.

Given the technological difficulties of approach 1, approach 2 is the most common solution adopted nowadays in the distributors in fin and tube heat exchangers (Fay, 2011) but also some developments can be found in the Literature following approach 1 (Hoesel, 1936).

In fin and tube heat exchangers, the problem of maldistribution of refrigerant is coupled with the problem of the maldistribution of air flow, leading frequently to an important deterioration of performance. A number of research studies have been dedicated to reduce this problem by either active flow control of the refrigerant flow through each refrigerant circuit (Kim et al. 2009), or by alternative designs of the refrigerant circuit (Bach et al., 2014; Bahman and Groll, 2017).

In microchannel heat exchangers, some use flow remedies to prevent separated flow along the inlet header (Jiang et al., 2010), and (Taras et al., 2010), or developing special nozzles to create a homogenous mist flow (Hrnjak, 2004). For this kind of heat exchangers, some solutions following approach 1 can also be found in the Literature, e.g. (Elbel and Hrnjak, 2004) proposed an improvement for achieving better refrigerant distribution based on this approach. The solution consisted of separating the liquid phase from the vapor phase after the expansion valve. In this way, only liquid is flowing to the microchannel heat exchanger while the vapor phase is being bypassed. Thermography pictures showed clearly a more uniformly distributed superheat with this flash gas removal system. Furthermore, better system performance was observed when using the separation device. Tuo and Hrnjak, (2013) revisited the refrigerant maldistribution problem in microchannel evaporators and highlighted the important effect of the pressure drop along the channels on the maldistribution.

Also active methods can be applied to improve the distribution. (Tingaud et al, 2013) showed that by using ultrasounds in the inlet manifold it is possible to significantly improve the distribution of a two-phase flow among vertical channels.

In Plate Heat Exchangers (PHE), the precise determination of the real refrigerant mass flowrate in each refrigerant channel is very difficult. Some research has been done in one phase flow in PHE. (Bassiouny and Martin, 1984a, 1984b) presented early studies on the influence of plate arrangements on flow distribution, their results indicated that the manifold diameter and number of channels have great influence in maldistribution. (Bobbili et al., 2006) analyzed experimentally the influence of the maldistribution in the thermal performance in PHE working in single-phase. (Thonon and Mercier, 1996) observed that Z-type plate arrangement have more tendency to suffer maldistribution. Regarding Brazed Plate Heat Exchangers (BPHE) not so many works can be found in the Literature. Among them it should be mentioned the one performed recently by (Li and Hrnjak, 2019) analyzing maldistribution in single phase flow.

Regarding two phase flow maldistribution in BPHEs, although the problem is well known (Jensen et al., 2015), and some solutions have been adopted by the main manufacturers in order to achieve a better refrigerant distribution, see for instance (SWEP, n.d.) where a system that feeds homogenously with refrigerant all channels has been developed, or the introduction of what is called equalancer distributor (Stenhede and Alfa Laval AB, 2008), from the practical point of view, there is not a definitive solution for this problem.

As mentioned before, infrared thermography has been used in order to study this phenomenon mainly in air to refrigerant heat exchangers, because its relatively easy access to the frontal area. (Bowers et al., 2010), or (Longo, 2010a, 2010b) used thermography in microchannel heat exchangers to visualize the two-phase flow region for different outlet vapor qualities and superheats of 5 and 10 K and to outline a methodology to quantify both refrigerant maldistribution and effective usage of the heat exchanger respectively.

In the present paper, the refrigerant maldistribution problem in a BPHE evaporator with a distributor is going to be analyzed as a function of the operating parameters: evaporator inlet vapor quality, evaporator superheat and water temperature drop across the evaporator, covering a wide range of their typical variation. This is the first time, that the refrigerant maldistribution has been studied systematically in a BPHE, and in such a large scope.

Part A includes the description of the experimental campaign, the obtained experimental results, and the results discussion. Part B includes an analysis of the degradation of the evaporation temperature due to the refrigerant maldistribution as well as of the influence of the other operating conditions, and additionally, a deeper analysis of the registered temperatures and of the causes for the great degradation observed when the water temperature drop is increased.

2. Experimental set-up test matrix

In order to proceed with evaporator characterization, a test bench for the characterization of water to water heat pumps was used. The test bench was able to control the water mass flowrate through the evaporator and the condenser in such a way that it allows maintaining a constant water temperature drop at a con-

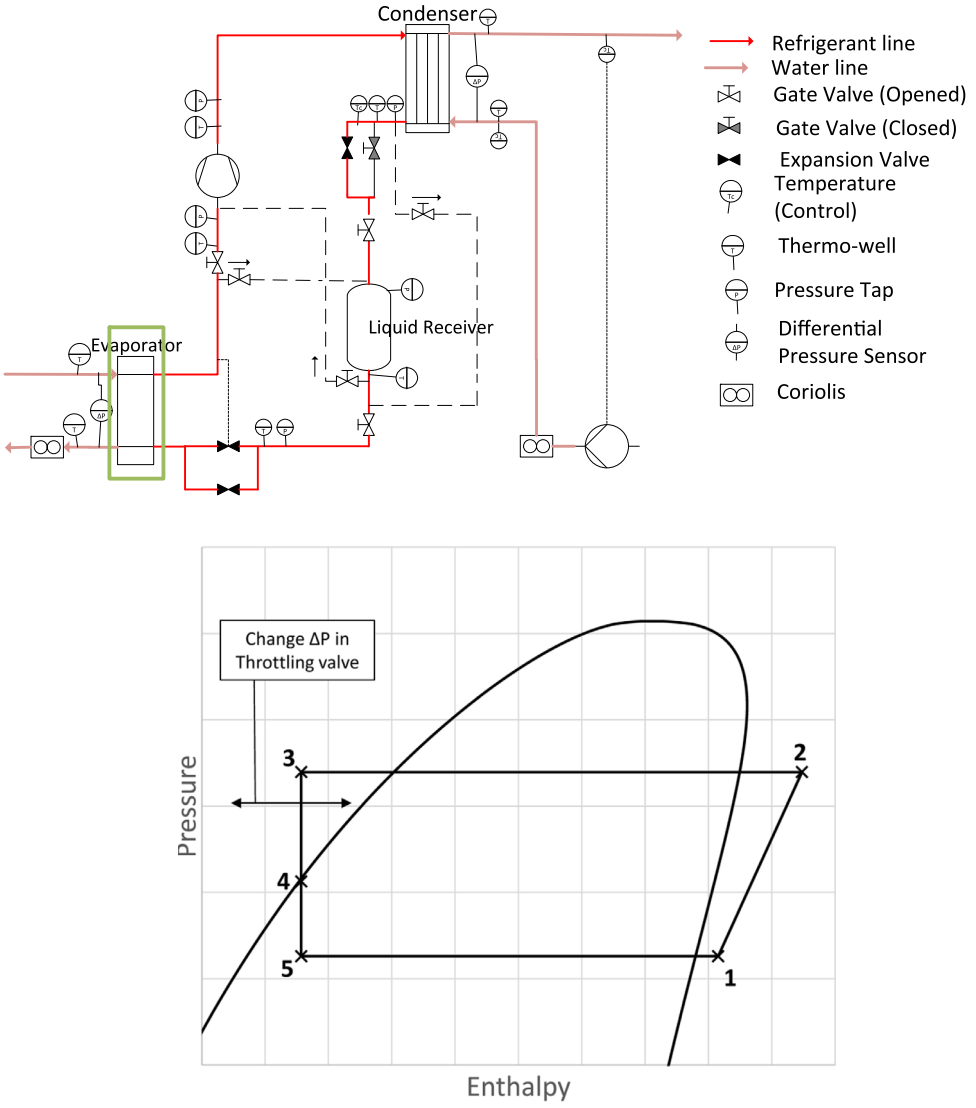

Fig. 1. System layout and refrigerant cycle

Table 1
Components of the heat pump system

Component	Type	Size
Compressor	Scroll (2900 rpm)	29.6 m^3h^{-1}
Condenser	BPHE Counter-flow	3.5 m^2
Evaporator	BPHE Counter-flow	6 m^2
Liquid receiver		8 l
Expansion valve	Electronic EX-6	93 kW
Throttling valve	Electronic EX-5	39 kW

stant inlet water temperature in both heat exchangers. The design and control of the heat pump allows to fix the subcooling and superheat independently. Table 1 shows the characteristics of the main components of the test bench. The system was operated with propane as refrigerant. The charge was about 5 kg, but we should point out that it was just a laboratory prototype not designed for minimum charge at all.

The layout of the heat pump is shown in Fig. 1 (dash lines of the circuit are not active for normal operation). Between the condenser and the liquid receiver there is a throttling valve, this valve allows the control of the subcooling at the outlet of the condenser and hence the vapor quality at the evaporator inlet. Its operation principle is shown in Fig. 1 (down); in steady state conditions, the liquid receiver must be in saturated conditions, this fact produces that changing the pressure drop introduced by the throttling valve, the system is able to control the amount of refrigerant inside the liquid receiver and the heat pump subcooling. Between the liquid receiver and the evaporator there is an electronic expansion valve which allows the control of superheat. Therefore, this experimental set up allows a stable control of the vapor quality at the evaporator inlet (subcooling at a condensing temperature) and the superheat at the evaporator outlet.

The system topology shown in Fig. 1 allows working in stable conditions at superheats higher than 5 K. In order to work in saturated conditions at the outlet of the evaporator, the circuit of the heat pump has to be modified in such a way that the liquid receiver is placed at the outlet of the evaporator, the throttling valve is then deactivated and the expansion valve controls subcooling instead of superheat. This configuration is able to fix the superheat at 0 K, while the only active control inside the heat pump is related with the subcooling and hence the evaporator inlet vapor quality.

The green box in Fig. 1 indicates the BPHE evaporator. The main characteristics of the evaporator are 120 plates, capacity of

Table 2
Instrumentation used in the test rig

	Model	Relative accuracy	Absolute accuracy
Pressure	P 1151 Smart GP7 Rosemount	0.12 % of Span	0.03 bar
	P 1151 Smart GP8 Rosemount	0.15 % of Span	0.08 bar
	P 3051 TG3 Rosemount	0.14 % of Span	0.04 bar
Temperature	RTD Class 1/10 DIN	-	0.06 K
Mass Flow	Coriolis SITRANS F C MASS 2100	0.3 % of Reading	
Thermography Camera	FLIR P640	0.3%	1 K

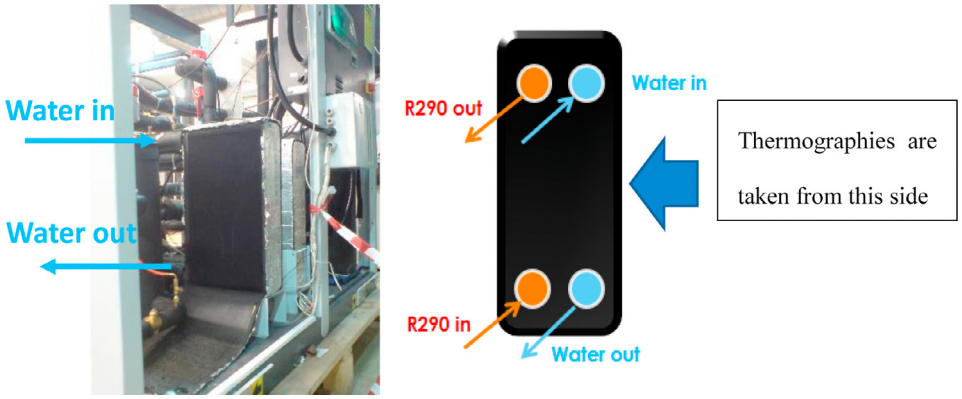

Fig. 2. Picture of a frontal view of the evaporator and a transversal view with the location of the inlet/outlet ports

40 kW at the nominal point, a horizontal port distance and vertical port distance of around 50 mm and 500 mm respectively, and approximately a 6 m^2 heat transfer area. The evaporator has orifices at the inlet of each refrigerant channel in order to minimize the refrigerant maldistribution.

Fig. 1 (up) also shows all the instrumentation used in the test unit. There is a water loop in the condenser and in the evaporator, each water loop has a temperature sensor at the inlet and outlet of the water side and have a Coriolis mass flow meter to measure the water mass flowrate. The water pumps of each circuit are equipped with an inverter which adjusts the water mass flowrate in such a way that the water temperature drop can be kept constant. More detailed information about this system can be found in (Hervás-Blasco et al., 2019).

Regarding the refrigerant circuit, two RTDs are placed in each inlet and outlet of both heat exchangers. Three pressure transducers are installed in the refrigerant side, at the compressor inlet and outlet and in the liquid receiver. This last pressure sensor constitutes a way to verify the subcooling value. The mass flowrate in the refrigerant side is determined by means of a heat balance between the water side and the refrigerant side. The relative and absolute accuracy of each device are shown in Table 2.

To investigate the refrigerant distribution, the temperature of the evaporator side was measured using a FLIR P640 infrared camera. The accuracy of the camera is shown in Table 2, it should be pointed out that although the estimation of the exact temperature has 1 K uncertainty, the sensibility of the camera is of 30 mK. The IR camera was set to a measuring range of -40 to 120°C.

Fig. 2 shows a picture of the evaporator installed in the system and a frontal view with the location of the refrigerant and water inlet/outlet ports. As it can be seen in the picture, the transversal side of the evaporator was covered with a non-reflective painting in order avoid any possible dispersion derived from undesired environmental radiation reflections. As can be seen, the infrared thermographies were taken of the side of the BPHE closer to the water inlet and outlet ports.

With this experimental setup and considering the possible factors having an influence in the refrigerant distribution, the refrigerant distribution in the evaporator was investigated for an evaporator outlet superheat (SH) ranging from 0 K to 15 K, an evaporator inlet quality (x) from around 0 to 0.3, and two different values of the water temperature drop across the evaporator(dTw) 5 and 13 K.

With the available experimental setup it was not possible to reach full liquid conditions at the inlet of the evaporator ($x = 0$). Of course, one could assume that in those conditions the distribution would be, if not completely even, very close to it, since the refrigerant liquid velocity is very low and so that the pressure drop along the port and distributor would also be low. Anyhow, we were able to perform, as indicated, a series of tests with low values of the inlet vapor quality, all close to 0.06.

The test matrix for the inlet vapor quality and the superheat is represented in Figure 3. Since the application of the heat pump unit was heat recovery from low temperature waste heat, water inlet temperature was always kept at 20°C. The testing campaign consisted of the repetition of the indicated matrix for two different values of the water temperature drop (dTw) across the evaporator: 5 and 13 K. The decision of taking 13 K, a value in between 10 and 15, was because we only wanted to have two levels for this parameter (5 and 13) and we wanted to cover a range similar to the one selected for the superheat (0–15). Nevertheless, as it will be described later on, we also performed some tests with a finer variation of this parameter in order to check the linearity of its effect on the evaporation temperature.

3. Experimental results

Table 3 and Table 4 show the corresponding IR thermographies for a water temperature drop across the evaporator of 5 K and 13 K respectively. The maximum temperature of the thermography scale is set to 20 °C since the water inlet temperature is always kept at that temperature, while the minimum is set to 5°C for the case of dTw = 5 and to -5°C for dTw = 13, what gives an adequate scale to distinguish the different regions for each case.

The values shown in the different columns represent different superheats and the values shown in the different rows represent

Table 3
Thermographies for dTw= 5 K with variation of inlet quality and superheat. Thermography scale 5°C/20°C

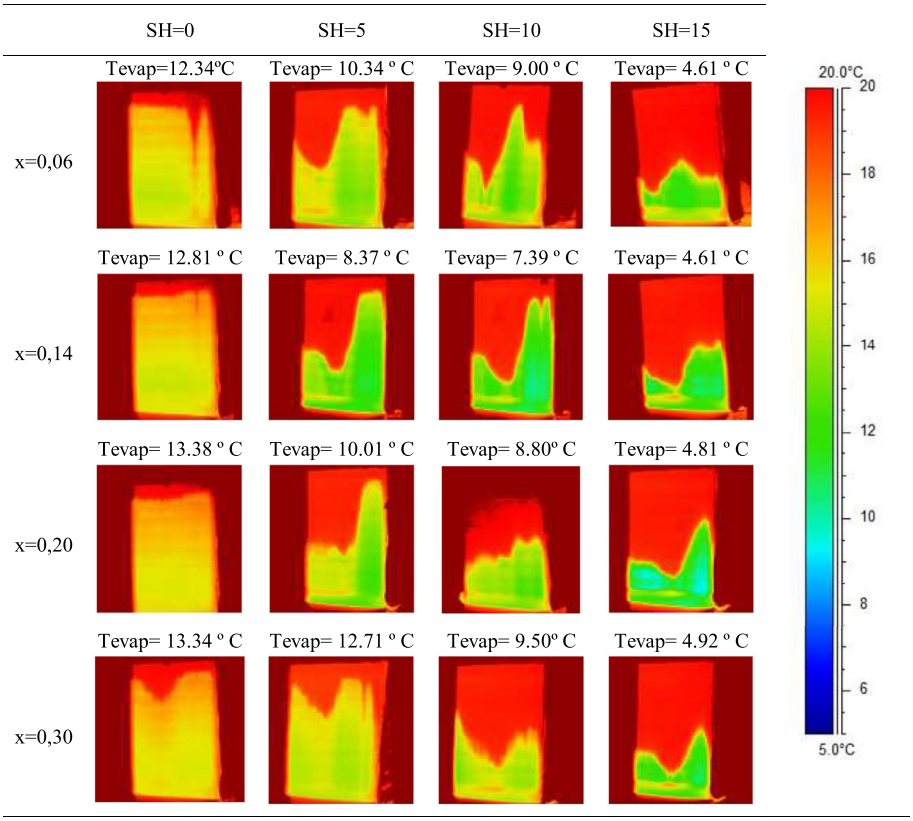

Table 4
Thermographies for dTw= 13 K with variation of inlet quality and superheat. Thermography scale -5°C/20°C

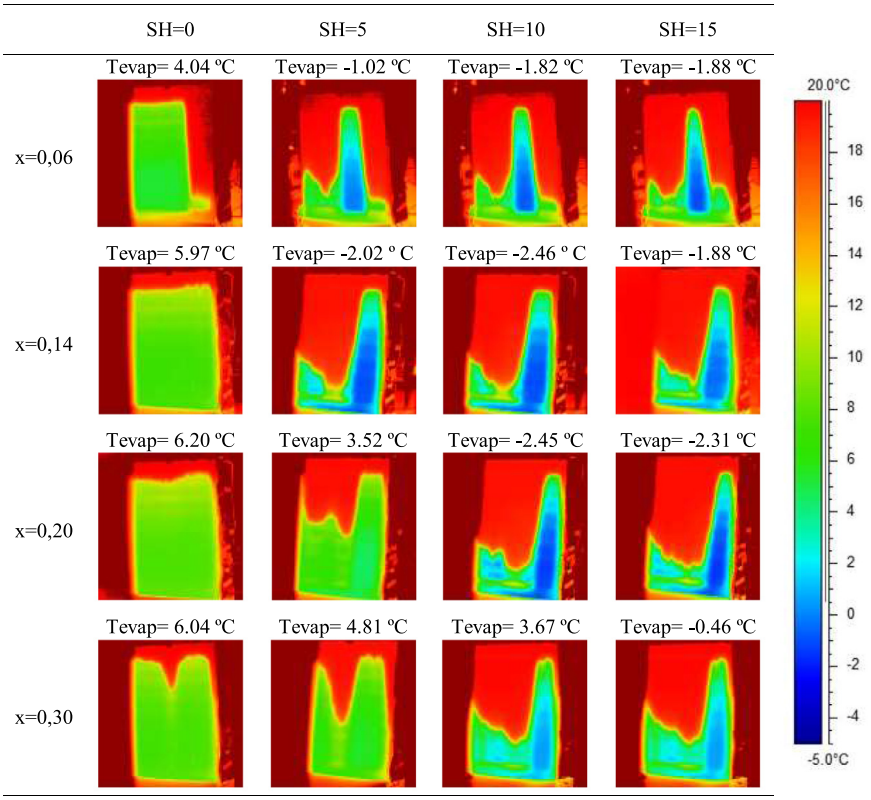

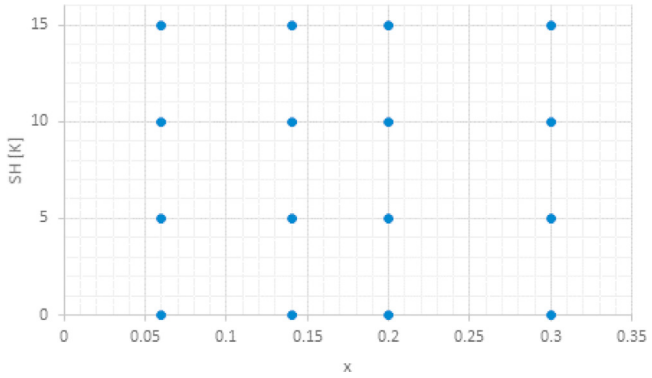

Fig. 3. Experimental test matrix for the inlet vapor quality x (-) and the superheat SH (K)

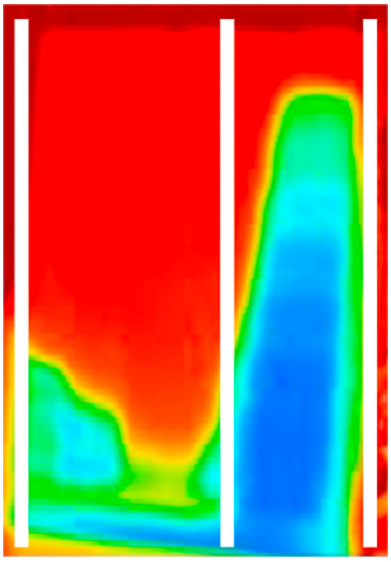

Figure 4. Hypothesized parts of the evaporator

different evaporator inlet qualities. It should be reminded that, both refrigerant and water, flow from left to right at their respective distribution channels, top for the water, bottom for the refrigerant. The refrigerant flows upwards, and the water downwards in countercurrent configuration. It should be noticed that the thermographies are taken of the side of the BPHE as indicated in Fig. 2, and that both top and bottom correspond to the inlet and outlet water distribution channels.

The measured evaporation temperature (T_{evap}) is shown on the top of each thermography.

The following observations can be made from the thermography pictures presented in Table 3 and Table 4:

The thermographies correspond to the lateral of the evaporator, where both water and refrigerant channels are brazed; therefore, it is difficult to know the influence of each fluid temperature on the registered temperatures. The temperature at the top is always very close to the water inlet temperature, 20°C. The evaporation temperatures at water temperature drop of 13 K are much lower than at 5 K.

The temperature fields in the case of null superheat are very different from the others, showing a much more uniform field, and no apparent degradation because maldistribution. Moreover, the evaporation temperatures with null superheat are much higher than the ones corresponding to higher superheats. Additionally, the evaporation temperatures at null superheat seem quite independent of the refrigerant inlet quality, with the lower values corresponding to the lower inlet qualities. This being explained by the fact that lower qualities mean a higher amount of liquid refrigerant to evaporate, therefore requiring lower evaporation temperatures.

At water temperature drop 13 K and the lowest inlet vapor quality, the final channels (right hand side) seem to have a very high temperature, possibly indicating a starvation of refrigerant.

The measured evaporation temperature is, very frequently, considerably lower than the temperatures registered at the bottom of each picture.

There are clearly marked areas with high temperatures, close to the water inlet temperature. Those areas increase with superheat. Both facts indicate that those are probably areas with a lot of vapor in the refrigerant channels and therefore the heat transferred to the water is very low. Those areas very probably correspond to dry out areas where the vapor is superheated, therefore, the rest of the areas should contain two-phase refrigerant flow, and it is where basically the evaporation takes place.

The two-phase flow region is clearly not even, showing a longer rise (with marked lower temperatures) at the right hand side. The end of this area at the top is, mostly, very close to the inlet distributor channel for the water, indicating that the evaporation is maybe not completed on those channels, and some refrigerant liquid is probably arriving to the outlet. This is always the case when the water temperature drop is 13 K for all the tested superheats and inlet qualities. However, when the water temperature drop is 5 K, the same tall area (with marked lower temperatures) on the right hand side is visible but it only seems to reach the top at low superheats. At higher superheats the area is still distinguishable but ends much before the top, indicating that all the refrigerant liquid has evaporated and above there is only vapor getting superheated. As it can be observed, the portion of channels with this pattern is approximately around 33%, globally.

The fact that this 33% of the channels is located at the right hand side, and that this region seem to have difficulties in evaporating all the circulating refrigerant, seem to prove that the refrigerant is not evenly distributed among the refrigerant channels, and that a good portion of the liquid refrigerant entering the evaporator is accumulating at the end of the distributor channel, at the right hand side of the evaporator, and flooding those channels with liquid refrigerant.

Fig. 4 shows a schematic with a fictitious division of the evaporator in two parts, the part on the right, which channels, as hypothesized, could be flooded with liquid refrigerant, and the one on the left, which channels have a higher vapor inlet quality and shows a large superheating area on the top. The thermography corresponds to the case with 13 K water temperature drop, inlet quality 0.14 and superheat 5 K.

As can be observed in Table 3 and 4, this distribution of the evaporator channels in two parts, which clearly seems to be correlated with the maldistribution of refrigerant among the channels, is not very influenced by the superheat. When the superheat increases, the superheated region of all channels tend to increase, but the distribution of channels is more or less the same.

The effect of the inlet quality on the maldistribution seems to be even weaker on the observed thermal profiles, except at the lowest inlet quality. At qualities close to 0.06, a more complex maldistribution appears with the flooded channels moving towards the center of the evaporator, and it seems, with a certain starvation of refrigerant of the end channels at the right.

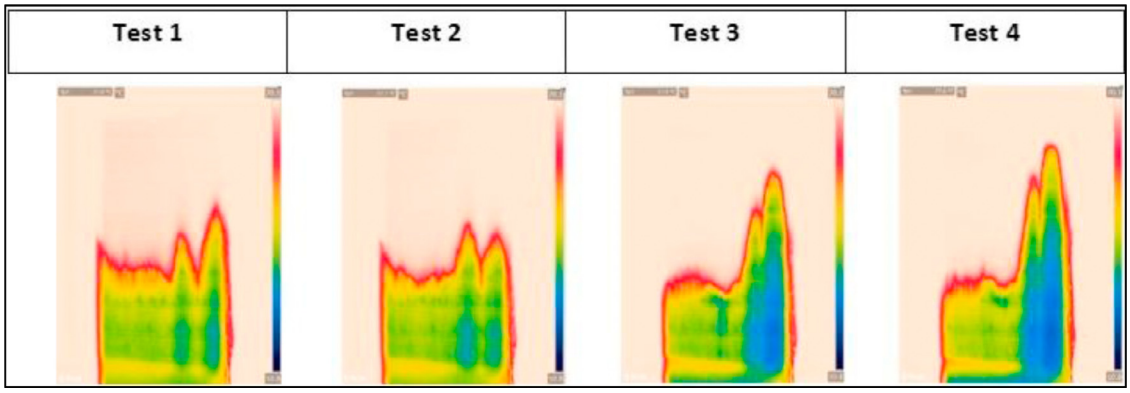

Fig. 5. Thermographies for several tests of the case with inlet vapor quality about 0.2, superheat 10 K and dTw = 5 K. Thermography Scale: 10°C/20°C.

Table 5
Registered measurements at several tests of the case with inlet vapor quality about 0.2, superheat 10 K and dTw = 5 K.

	Test 1	Test 2	Test 3	Test 4	Absolute uncertainty
dTw (K)	4.83	4.76	4.71	4.67	0.4
Tevap (°C)	9.26	8.80	8.78	8.72	0.2
Tcond (°C)	44.6	44.8	45.0	45.1	0.2
Xin (-)	0.195	0.199	0.200	0.198	0.003
SH (K)	10.6	11.0	10.4	10.3	0.4
Ref. mass flowrate (kg s^{-1})	0.1017	0.1002	0.1000	0.0993	0.0004

A number of tested points were repeated, always showing the same results. However, at inlet vapor quality about 0.2 and superheat 10 K for the case with water temperature drop of 5 K a certain variation of the maldistribution was observed, and therefore the tests were repeated several times.

Fig. 5 shows the corresponding thermographies, and Table 5 the values of the registered data. As can be observed, the values of the operating conditions are very close to each other. However, as can be seen in Fig. 5, it seems that for this case there are two possible distributions for the refrigerant among the channels. Tests 3 and 4 present the same maldistribution seen in most of the cases, with refrigerant liquid accumulating at the end channels. However, tests 1 and 2 show a more even distribution, with also some accumulation at the end channels but of lower intensity. It should be pointed out that the distribution of tests 3 and 4 are much similar than the other ones to the tests with the same conditions but lower (5 K) or higher superheat (15 K), as can be seen in Table 3. Anyhow, the influence of maldistribution at these conditions seems to have very little effect on the evaporator performance, since, as it can be seen in Table 5, the registered values of evaporation temperature are very close to each other, with just slightly higher values for tests 1 and 2, which are consistent with a clearly better refrigerant distribution. Tests number 1 to 4 were done trying to approach the operating conditions in a different way each one. It is obvious that the way to approach the test point had an influence on the distribution of the refrigerant. However, no correlation between the way and the result was found. This phenomenon of variation of the distribution was only observed at this point and, interestingly, at the same conditions but with dTw = 13 K, with very similar characteristics, although with a higher influence on the resulting evaporation temperature.

These obsevations seem to indicate some kind of hysteresis which we interpreted could be caused by how the refrigerant liquid is actually distributed at the distribution header (at the bottom of the heat exchanger) before changing the operation point, meaning that when you change the operating conditions the new distribution you get could depend on the initial distribution of the liquid that was obtained in the previous test point. In any case, as mentioned above, the registered variation of the evaporation temperature was always small, just the thermography appeared a bit different.

4. Evaporation temperature

Fig. 6 presents the measured evaporation temperature as a function of the inlet vapor quality and superheat for the water temperature drops (dTw) of 5 K (blue surface) and 13 K (green surface) respectively. Two different views (left, and right) are shown in order to allow a better understanding of the shape of the surfaces. The surfaces are generated after applying a TPS (Thin Plate Spline gridding) interpolation technique, basically consisting in bending a surface in a way that it adapts to the experimental points (Donato and Belongie, 2002). The measured points are indicated as dots. It can be observed that the surface is very close to all points but it is not forced to pass exactly through the experimental points.

As it can be clearly distinguished in Fig. 6, the evaporation temperature first depends on the water temperature drop across the evaporator, with very much lower values at dTw = 13 K. The shape of the surfaces is also different. Both have a trend to decrease with superheat, with a sudden decrease from null superheat. At dTw = 13 K, also the inlet vapor quality seems to have a strong effect with a decreasing trend as the quality is decreased. This trend is not the same at dTw = 5 K, showing a valley shape with minimum values at intermediate qualities.

In order to verify the variation of the evaporation temperature with the water temperature drop, a set of additional tests were performed for the conditions of X = 0.14 and superheats 5 K and 10 K. Fig. 7 presents the corresponding thermographies and the evaporation temperature vs. the water temperature drop for superheats 5 K and 10 K. First, it can be seen that the shape of the thermographies is more or less the same, with a higher superheated region logically at superheat 10. The distribution in two evaporator parts, as described, is clearly present, with greatest differences between them at the higher dTw. The evaporation temperature decreases more or less monotonously with dTw, with a

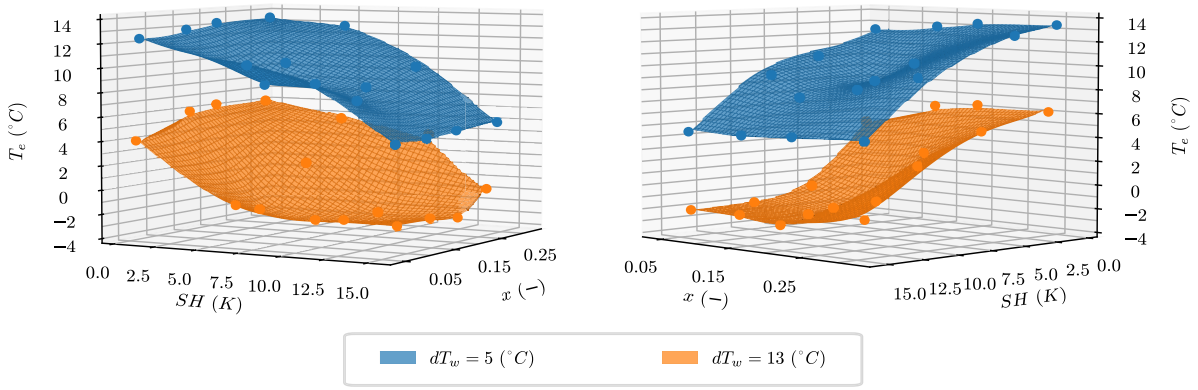

Fig. 6. Measured evaporation temperature vs. superheat and inlet vapor quality, for dTw = 5 K, and dTw = 13 K.

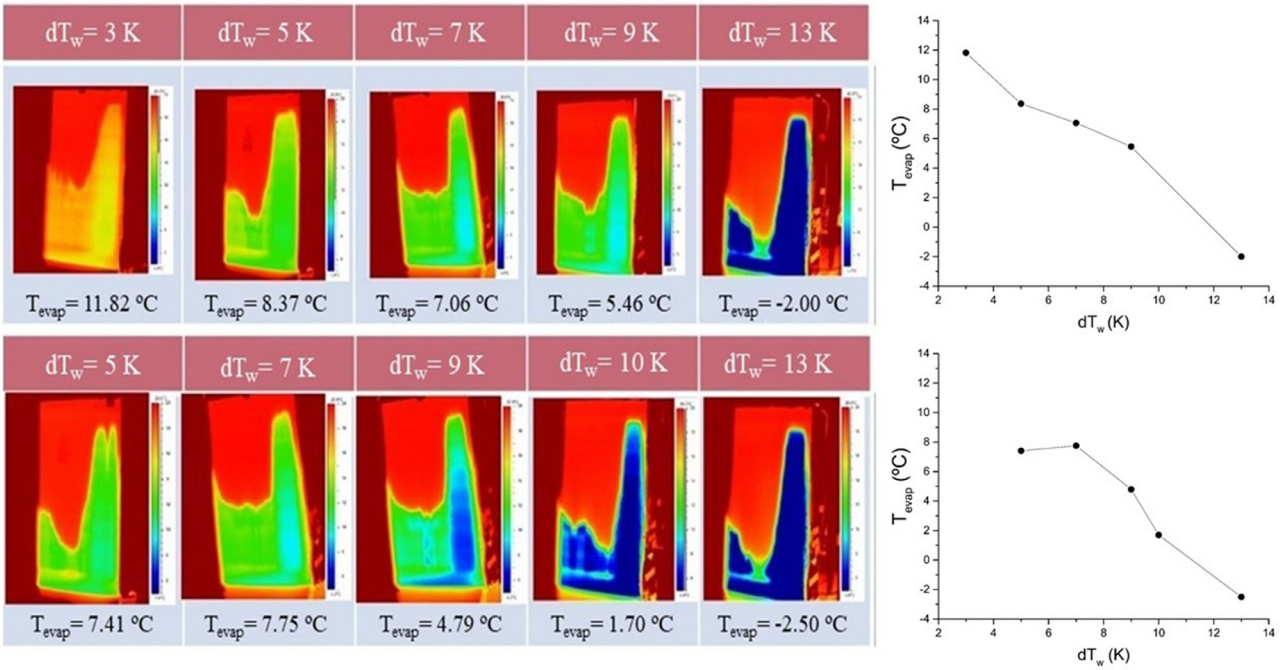

Fig. 7. Evolution of evaporating temperature as a function of the water temperature drop for superheats 5 K and 10 K, and 0.14 inlet vapor quality.

sharper drop at superheat around 7 K for SH = 5 K, and around 8 K for SH = 10 K. Therefore, it seems that the temperature drop of the water across the evaporator has a clear influence on the evaporation temperature but has little effect on the refrigerant maldistribution.

In order to better understand the influence of the operation conditions on the evaporation temperature, Fig. 8 shows the evaporation temperature isoline-maps corresponding to the two tested water temperature drops. The temperature scale is the same for both cases, ranging from the lowest to the highest registered evaporation temperatures (-3.25 °C to 13.4 °C). Again, the first thing to highlight is the great differences in evaporation temperatures depending on the operating conditions and mainly on the water temperature drop across the evaporator.

The minimum evaporation temperature at dTw = 13 K is -3.25 °C and it is located approximately at an inlet vapor quality of 0.15 and superheat 8 K. Minimum evaporation temperatures at dTw = 5 K are find at the highest superheats with values around 5°C, but there is a local minimum around 9 °C located approximately at an inlet vapor quality of 0.15 and superheat 6 K. As it can be observed in Fig. 8 (left) at dTw = 5 K, the evaporation temperature mainly depends on the superheat with a general trend to decrease as the superheat increases. This effect is natural in all evaporators since the superheat needs a temperature difference between the water inlet temperature (20°C in this case) and the evaporation temperature, at least higher than the required superheat. However, some effect of the vapor inlet quality is clearly seen with lower values of the evaporation temperatures around vapor qualities about 0.15. In contrast, The influence of vapor quality and superheat at dTw = 13 K are both important with a very sudden drop of evaporation temperature for superheats greater than 5 K and vapor qualities lower than 0.3, forming a plateau with very low evaporation temperatures.

Finally, it should be pointed out that the refrigerant mass flowrate was not kept constant in this study because we wanted to take into account the influence that the evaporation temperature has on the compressor mass flowrate. Therefore, all tests were performed with the compressor running at fixed speed. Condensation temperature was left to vary depending on the refrigerant flowrate. In this way, the influence of the evaporation temperature on the refrigerant mass flowrate is very close to the one occurring during the actual operation of the system.

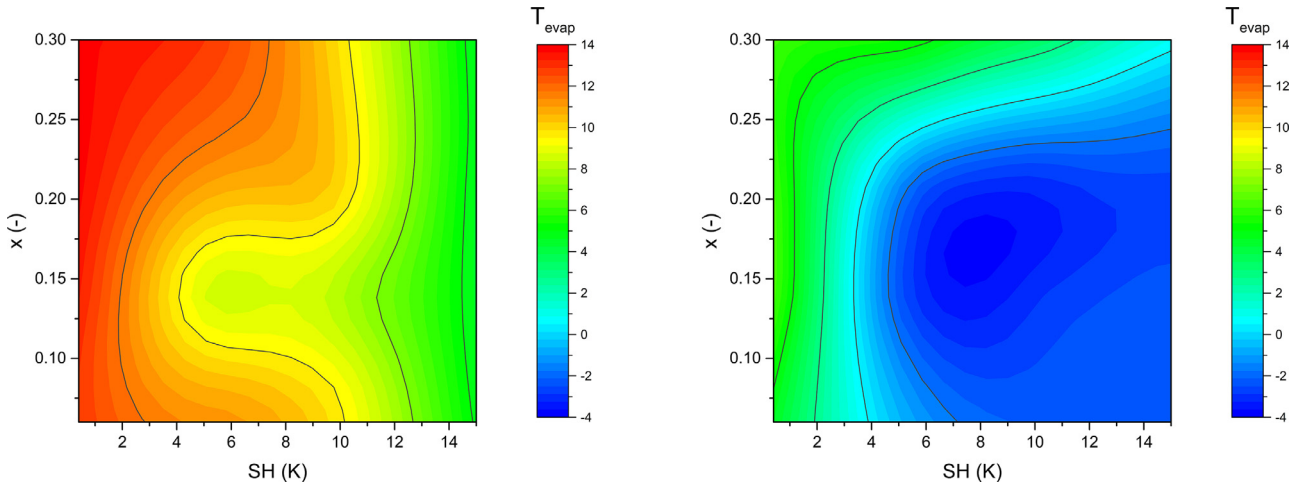

Fig. 8. Measured evaporation temperature map in °C with isolines vs. superheat and inlet vapor quality, for dTw = 5 K (left), and dTw = 13 K (right).

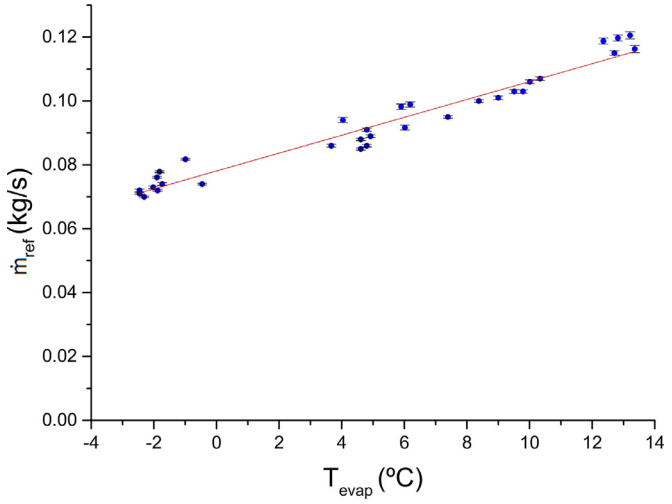

Fig. 9. Measured refrigerant mass flowrate (with the corresponding uncertainty bars) vs. evaporation temperature

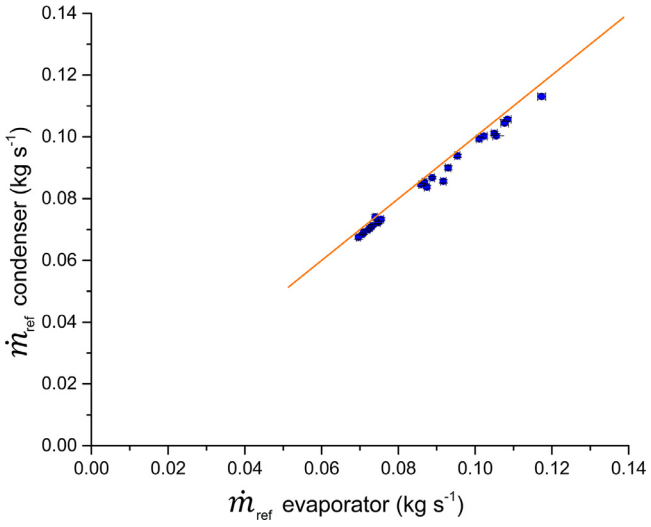

Fig. 10. Refrigerant mass flowrate estimated from the heat balance at the condenser vs. the refrigerant mass flowrate estimated from the heat balance at the evaporator, with the corresponding uncertainty bars.

Fig. 9 shows the evaporation temperature results versus the corresponding refrigerant mass flowrate. As it can be observed, there is a quite linear increasing dependence between the mass flowrate and the evaporation temperature. This slope mainly corresponds to the combined effect of the increase of refrigerant density at the compressor suction, and the reduction of the pressure ratio, when evaporation temperature increases. The scattering around the trend line is mainly due to the variation of the compressor flowrate because of the variation of the condensation pressure and of the superheat.

Fig. 9 demonstrates that if the evaporation temperature is low in some conditions, it is not due to a variation of the refrigerant mass flowrate since a decrease of the mass flowrate will lead to an increase of the evaporation temperature. For the same reason, it means that if the tests would have been performed at constant refrigerant flowrate the observed degradation of the evaporation temperature would have been greater.

The refrigerant mass flowrate was estimated from the heat balance at the condenser, and at the evaporator, as the average between both estimated values. Fig. 10 shows the comparison between both values including the corresponding error bars. As it can be observed the estimated values from both heat exchangers agree well.

5. Conclusions

The refrigerant distribution in a BPHE evaporator with distributor has been studied with a thermographic camera working under different conditions of inlet vapor quality, superheat, and water temperature drop. The thermographies have shown a clear uneven thermal distribution except when superheat is null. The temperature field in the case of null superheat is quite uniform, and the evaporation temperatures are much higher than in all other cases, with little influence of the inlet quality.

The thermographies when there is a superheat, show that probably a great part of the liquid accumulates at the end channels of the evaporator and most of the vapor remains in the first channels. The distribution of channels, although with different shapes is the following: approximately 2/3 of the channels seem to have little refrigerant liquid, and hence a high inlet vapor quality, showing a high temperature region on the top which probably corresponds to a dry out area with superheating of the vapor; the other 1/3 of the channels seem to be fed mostly by refrigerant liquid, rising almost up to the outlet distributor and clearly showing much lower temperatures.

This distribution of channels in two parts seems quite independent of both superheat or inlet quality, with the exception of low qualities, where a more complex distribution appears.

Some lack of repeatability of the results was detected at some special operation conditions. The tests were repeated several times at those points, showing that although the evaporation temperature was not very affected, the distribution of the refrigerant among the channels could adopt two different solutions, depending probably on how the test point was approached. That means that it could exist some hysteresis in the way the liquid and vapor refrigerant is distributed among the channels.

The registered evaporation temperatures are much lower for the case of 13 K of water temperature drop across the evaporator, highlighting the importance of the influence of the water mass flowrate on the evaporator performance. Therefore, it is clear that the temperature drop of the water across the evaporator has an important influence on the evaporation temperature, however it seems to have little effect on the refrigerant maldistribution.

Based on the obtained results, it can be concluded that applications in which the evaporator works with water temperature drops higher than usual, like waste heat recovery applications, can be especially affected by the problem of refrigerant maldistribution with a considerable penalty on the evaporation temperature.

Part B of this study includes an analysis of the degradation of the evaporation temperature due to the refrigerant maldistribution as well as a deeper analysis of the registered temperatures and of the causes for the great degradation observed when the water temperature drop is increased.

Declaration of Competing Interest

The authors declare that they have no known competing financial interests or personal relationships that could have appeared to influence the work reported in this paper.

Acknowledgments

The authors would like to acknowledge the Spanish 'Ministerio de Economia Y Competitividad', through the project "Maximizacion de la Eficiencia Y Minimizacion del Impacto Ambiental de Bombas de Calor Para la Descarbonizacion de la Calefaccion/ACS en los Edificios de Consumo Casi Nulo" with the reference ENE2017-83665-C2-1-P for the given support.

Supplementary materials

Supplementary material associated with this article can be found, in the online version, at doi:10.1016/j.ijrefrig.2021.04.002.

References

Bassiouny, M.K., Martin, H., 1984a. Flow distribution and pressure drop in plate heat exchangers—I U-type arrangement. Chem. Eng. Sci. 39, 693–700. doi:10.1016/0009-2509(84)80176-1.

Bassiouny, M.K., Martin, H., 1984b. Flow distribution and pressure drop in plate heat exchangers—II Z-type arrangement. Chem. Eng. Sci. 39, 701–704. doi:10.1016/0009-2509(84)80177-3.

Bach, C.K., et al., 2014. Mitigation of air flow maldistribution in evaporators. Appl. Therm. Eng. 73, 879–887. doi:10.1016/j.applthermaleng.2014.08.010.

Bahman, A.M., Groll, E., 2017. Application of interleaved circuitry to improve evaporator effectiveness and COP of a packaged AC system. Int.J.Refrig 79, 114–129. doi:10.1016/j.ijrefrig.2017.03.026.

Bobbili, P.R., Sunden, B., Das, S.K., 2006. An experimental investigation of the port flow maldistribution in small and large plate package heat exchangers. Appl. Therm. Eng. 26, 1919–1926. doi:10.1016/J.APPLTHERMALENG.2006.01.015.

Bowers, C.D., Wujek, S.S., Hrnjak, P., 2010. Quantification of refrigerant distribution and effectiveness in microchannel heat exchangers using infrared thermography. Refrig. Air Cond. 1–8.

Donato, G., Belongie, S., 2002. Approximation methods for thin plate spline mappings and principal warps. In: 7th Eur. Conf. Comput. Vision-Part III, 94063, pp. 21–31.

Elbel, S., Hrnjak, P., 2004. Flash gas bypass for improving the performance of transcritical R744 systems that use microchannel evaporators. Int. J. Refrig. 27, 724–735. doi:10.1016/J.IJREFRIG.2004.07.019.

Fay, M.A., 2011. Effect of conical distributors on evaporator and system performance. (Doctoral dissertation).

Hervás-Blasco, E., Navarro-Peris, E., Barceló-Ruescas, F., Corberán, J.M., 2019. Improved water to water heat pump design for low-temperature waste heat recovery based on subcooling control | Conception d'une pompe à chaleur eau-eau optimisée pour la récupération de chaleur perdue à basse température basée sur la régulation du sous-re. Int.J.Refrig 106, 374–383. doi:10.1016/j.ijrefrig.2019.06.030.

Hoesel, A.F., 1936. Refrigerant distributor. U.S. Patent No. 2,063,380. U.S. Patent and Trademark Office, Washington, DC.

Hrnjak, P., 2004. Developing adiabatic two phase flow in headers - distribution issue in parallel flow microchannel heat exchangers. Heat Transf. Eng. 25, 61–68. doi:10.1080/01457630490280128.

Jensen, J.K., Kærn, M.R., Ommen, T., Markussen, W.B., Reinholdt, L., Elmegaard, B., 2015. Effect of liquid/vapour maldistribution on the performance of plate heat exchanger evaporators. In: Refrigeration Science and Technology, pp. 2007–2014. doi:10.18462/iir.icr.2015.0550.

Jiang, J., Lu, X., Huang, L., 2010. Refrigerant distributor for heat exchanger. US Pat. No 20100242535 A 1, 2010.

Kim, J.H., Braun, J., Groll, E., 2009. A hybrid method for refrigerant flow balancing in multi-circuit evaporators: Upstream versus downstream flow control. Int.J.Refrig 32, 1271–1282. doi:10.1016/j.ijrefrig.2009.01.013.

Li, W., Hrnjak, P., 2019. Experimental investigations of the single-phase flow distribution in brazed plate heat exchangers and its impact on the heat exchanger. Refrig. Sci. Technol. 2746–2753. doi:10.18462/iir.icr.2019.1564.

Longo, G.A., 2010a. Heat transfer and pressure drop during HFC refrigerant saturated vapour condensation inside a brazed plate heat exchanger. Int. J. Heat Mass Transf. 53, 1079–1087. doi:10.1016/J.IJHEATMASSTRANSFER.2009.11.003.

Longo, G.A., 2010b. HC-290 (Propane) Vaporisation Inside a Brazed Plate Heat Exchanger. Int. Refrig. Air Cond. Conf. 1009.

Madanan, U., Nayak, R., Chatterjee, D., Das, S.K., 2018. Experimental investigation on two-phase flow maldistribution in parallel minichannels with U-type configuration. Can. J. Chem. Eng. 96, 1820–1828. doi:10.1002/cjce.23112.

Taras, M.F., Kirkwood, A.C., Chopko, R.A., 2010. Parallel flow evaporator with spiral inlet manifold. U.S. Patent No 7806171.

Thonon, B., Mercier, P., 1996. Les échangeurs à plaques: dix ans de recherche au GRETh: Partie 2. Dimensionnement et mauvaise distribution. Rev. Générale Therm. 35, 561–568. doi:10.1016/S0035-3159(99)80082-8.

Tingaud, F. Ferrouillat, S. Colasson, Bulliard-Sauret, O. Bontemps, A. (2013). Improvement of two-phase flow distribution in compact heat exchangers by using ultrasound. applied mechanics and materials. 392. 521–525. 10.4028/www.scientific.net/AMM.392.521.

Tuo, H., Hrnjak, P., 2013. Effect of the header pressure drop induced flow maldistribution on the microchannel evaporator performance. Int. J. Refrig. 36, 2176–2186. doi:10.1016/j.ijrefrig.2013.06.002.

Vist, S., Pettersen, J., 2004. Two-phase flow distribution in compact heat exchanger manifolds. Exp. Therm. Fluid Sci. 28, 209–215. doi:10.1016/S0894-1777(03)00041-4.

Zou, Y., Hrnjak, P.S., 2013. Refrigerant distribution in the vertical header of the microchannel heat exchanger – Measurement and visualization of R410A flow. Int. J. Refrig. 36, 2196–2208. doi:10.1016/J.IJREFRIG.2013.04.021.